Available online at www.sciencedirect.com
ScienceDirect
Journal of Sound and Vibration 299 (2007) 1114–1123
JOURNAL OF SOUND AND VIBRATION
www.elsevier.com/locate/jsvi

Short Communication

# Propagation constants of railway tracks as a periodic structure

X. Sheng*, M.H. Li

*Civil Engineering Department, East China Jiaotong University, Nanchang, Jiangxi, 330013, China*

Received 10 April 2006; received in revised form 8 July 2006; accepted 7 August 2006
Available online 2 October 2006

**Abstract**

This short communication serves two purposes: (1) to demonstrate the usefulness of a previously derived, much more general, propagation constant equation by producing propagation constant curves for two one-dimensional periodic structures, an infinitely long Euler beam on simple supports and a conventional ballasted railway track; and (2) to present a detailed discussion on the propagation and resonance properties of the track, which may be helpful to understand the track dynamics and useful in modelling wheel/rail interaction problems.


## 1. Introduction

It is important to have the knowledge of free vibration propagation in railway tracks as a periodic structure in calculating rail-radiated noise and wheel/rail interactions. Free vibration in one-dimensional (1D) periodic structures is characterised by the frequency-dependent propagation constant, $\varepsilon$, which satisfies $\{q(x+l,t)\} = \{q(x,t)\}e^{i\varepsilon}$ [1] for any position $x$ and time $t$, where, $i = \sqrt{-1}$, $\{q(x,t)\}$ denotes the displacement vector of the free vibration at cross-section $x$ and time $t$, and $l$ is the period of the structure. Some 1D periodic structures, like a railway track, can be regarded as a main structure (e.g., the rail of a track) to which an infinite number of 'supports' (e.g., railpad/sleeper/ballast) are attached at a given spacing $l$. Two methods are often used to calculate the propagation constant: the receptance method and the transfer matrix method [1]. The first method is normally applied in an analytical way and therefore restricted to simple main structure models. With the finite element method involved, the transfer matrix method can account for more complex main structures but leads to heavy computations because of the necessary longitudinal discretization. Efforts to overcome this shortcoming are made in Ref. [2] in which displacement variation of the main structure in the longitudinal direction is synthesised using some sort of modes. Recently, a general equation is derived as a by-product in Ref. [3] for calculating the propagation constant. This equation applies to any main structure which is uniform in the longitudinal direction but the cross-section can have any shape. The supports, described by a receptance matrix, may have arbitrary degrees of freedom (dof), either translational or rotational. However, no result from this general equation is shown in that paper, since that paper serves a different purpose.

*Corresponding author. Applied Mechanics Group, Technical Centre, Cummins Turbo Technologies Ltd, St Andrew's Road, Huddersfield, HD1 6RA, England. Tel.: +0044 1484 440522.
*E-mail address:* shengxiaozhen@hotmail.com (X. Sheng).

0022-460X/$ - see front matter © 2006 Elsevier Ltd. All rights reserved.
doi:10.1016/j.jsv.2006.08.010

To demonstrate its usefulness, this short communication applies this general equation to produce propagation constant curves, first for an Euler beam on periodically repeated simple supports, and then for a conventional ballasted track. The propagation constant curves are presented in Section 2. Using the propagation constant curves of the track, this short communication also presents, in Section 3, a detailed discussion and explanation on the dynamic behaviour of the track, raising issues which should be taken into account when modelling high frequency, high train speed wheel/rail interaction problems.

## 2. Propagation constant equation and applications

### 2.1. Propagation constant equation for 1D periodic structures

First, the propagation constant equation derived in Ref. [3] is briefly described here, in a slightly different version. Note that the equation is derived in terms of *propagation wavenumber* $\beta$ instead of propagation constant $\varepsilon$; they are related by $\beta = \varepsilon/l$.

Using the 2.5D finite element method, the free vibration, $\{q(x,t)\} = \{\tilde{q}(x)\}\,\mathrm{e}^{\mathrm{i}\omega t}$ at $x$ cross-section and at time $t$, of the main structure without any support, is governed by the following equation [4]

$$[\mathbf{M}]\frac{\partial^2\{q(x,t)\}}{\partial t^2} + [\mathbf{K}]_0\{q(x,t)\} + [\mathbf{K}]_1\frac{\partial\{q(x,t)\}}{\partial x} + [\mathbf{K}]_2\frac{\partial^2\{q(x,t)\}}{\partial x^2} + [\mathbf{K}]_3\frac{\partial^3\{q(x,t)\}}{\partial x^3} + [\mathbf{K}]_4\frac{\partial^4\{q(x,t)\}}{\partial x^4} = 0, \tag{1}$$

where $[\mathbf{M}]$ etc. are constant matrices of order $N \times N$ with $N$ being the dof of a cross-section. If denoting

$$[\mathbf{D}(\beta,\omega)] = -\omega^2[\mathbf{M}] + [\mathbf{K}]_0 + \mathrm{i}\beta[\mathbf{K}]_1 - \beta^2[\mathbf{K}]_2 - \mathrm{i}\beta^3[\mathbf{K}]_3 + \beta^4[\mathbf{K}]_4, \tag{2}$$

then the dispersion equation of the free main structure is given by

$$\det[\mathbf{D}(\beta,\omega)] = 0, \tag{3}$$

where $\beta$ is the wavenumber in the $x$-direction at (radian) frequency $\omega$.

Now identical supports are attached to the main structure at $x = 0, \pm l, \pm 2l, \ldots$ to form the periodic structure under investigation. Associating with the dof of the main structure at a cross-section where a support is attached, the support may be described by a receptance matrix $[\mathbf{H}(\omega)]$ of order $N \times N$. The vector, $\{\tilde{F}_j(\omega)\}$, constructed from the amplitudes of the forces applied by the main structure to the support, can be related to the displacement amplitude vector of the main structure at $x = jl$, that is $\{\tilde{q}(jl)\}$, via $[\mathbf{H}(\omega)]$, i.e.,

$$\{\tilde{q}(jl)\} = [\mathbf{H}(\omega)]\{\tilde{F}_j(\omega)\}. \tag{4}$$

Now define

$$\beta_j = \beta - \frac{2\pi j}{l}, \tag{5}$$

$$[\mathbf{D}(\beta_j,\omega)] = -\omega^2[\mathbf{M}] + [\mathbf{K}]_0 + i\beta_j[\mathbf{K}]_1 - \beta_j^2[\mathbf{K}]_2 - i\beta_j^3[\mathbf{K}]_3 + \beta_j^4[\mathbf{K}]_4, \tag{6}$$

$$[\mathbf{A}(\beta,\omega)] = \frac{1}{l}\sum_{j=-\infty}^{\infty}[\mathbf{D}(\beta_j,\omega)]^{-1} + [\mathbf{H}(\omega)]. \tag{7}$$

Then according to Eq. (47) of Ref. [3] the propagation wavenumber equation of the periodic structure is given by

$$\det([\mathbf{A}(\beta,\omega)]) = 0, \tag{8}$$

i.e., for a given frequency $\omega$, the real root of Eq. (8) is the corresponding propagation wavenumber of the periodic structure. It can be seen that matrix $[\mathbf{A}(\beta,\omega)]$ in Eq. (7) is a periodic function of $\beta$ with period equal to $2\pi/l$; therefore if $\bar{\beta}$ is a real root of Eq. (8), then $\bar{\beta} - (j2\pi/l)$ $(j = \pm 1, \pm 2, \ldots)$ are roots as well.

If the eigen vector of matrix $[\mathbf{A}(\beta,\omega)]$ is denoted by $\{\phi\}$ for eigen value $\bar{\beta}$ (i.e., $\bar{\beta}$ is a real root of Eq. (8)), then the free vibration in the main structure is given by (Eq. (48) in Ref. [3])

$$\{q(x,t)\} = \sum_{j=-\infty}^{\infty} \left[\mathbf{D}(\bar{\beta}_j,\omega)\right]^{-1}\{\phi\}\, \mathrm{e}^{\mathrm{i}\bar{\beta}_j x}\, \mathrm{e}^{\mathrm{i}\omega t}, \tag{9}$$

where $\bar{\beta}_j = \bar{\beta} - 2\pi j/l$. It can be seen that the free vibration in the main structure consists of an infinite number of spatially harmonic waves at wavenumbers $\bar{\beta}_j = \bar{\beta} - j2\pi/l$. If there is a $j$ such that $\bar{\beta}_j$ is close to a wavenumber of the free main structure (i.e., without supports) then $\det[\mathbf{D}(\bar{\beta}_j,\omega)] \approx 0$ (see Eq. (3)). In this case, as indicated in Eq. (9), the free vibration of the main structure is dominated by the harmonic wave at wavenumber $\bar{\beta}_j$.

The periodic structure becomes a continuously supported structure if the dynamic stiffness matrix (which is the inverse of the receptance matrix) of a support is evenly distributed along a bay (i.e., dividing the dynamic stiffness matrix by $l$). Such a continuously supported model is often adopted for railway tracks in the past. For the continuous support, the displacement due to a unit force per unit length is given by $l[\mathbf{H}(\omega)]$. The propagation wavenumber of the continuously supported structure at frequency $\omega$ is given by [3]

$$\det([\mathbf{A}_0(\beta,\omega)]) = \det\left([\mathbf{D}(\beta,\omega)]^{-1} + l[\mathbf{H}(\omega)]\right) = 0, \tag{10}$$

and the propagating wave is a purely harmonic wave at wavenumber $\beta$.

### 2.2. Propagation constant curves of an Euler beam on simple supports

In this sub-section, propagation constants of an Euler beam on simple, periodically repeated supports are produced using Eq. (8) and compared with those calculated from a propagation constant equation [1] which has a closed form but is specific to this particular periodic structure. The differential equation of motion of the free beam is given by

$$EI\frac{\partial^4 q(x,t)}{\partial x^4} + m\frac{\partial^2 q(x,t)}{\partial t^2} = 0, \tag{11}$$

where $EI$ is the bending stiffness and $m$ the mass per unit length of the beam. The receptance of a simple support is zero. According to Eqs. (7) and (8), the propagation wavenumber of this periodic structure at frequency $\omega$ satisfies,

$$A(\beta,\omega) = \sum_{j=-\infty}^{\infty} \frac{1}{EI(\beta - 2\pi j/l)^4 - m\omega^2} = 0. \tag{12}$$

The free vibration of the beam at propagation wavenumber $\bar{\beta}$ is given by

$$q(x,t) = \sum_{j=-\infty}^{\infty} \frac{1}{EI(\bar{\beta} - 2\pi j/l)^4 - m\omega^2}\, \mathrm{e}^{\mathrm{i}(\bar{\beta}-2\pi j/l)x}\mathrm{e}^{\mathrm{i}\omega t}. \tag{13}$$

Eq. (13) shows that, at supports where $x = 0, \pm l, \pm 2l, \ldots$, the displacement is guaranteed to vanish by Eq. (12).

The real roots of Eq. (12) may be obtained numerically. Alternatively, the contour plot of $1/|A(\beta,\omega)|$ on the frequency–wavenumber plane may be used to produce propagation constant curves, as shown in Fig. 1 (in yellow). To be comparable with results in Ref. [1], frequency has also been normalised; the non-dimensional frequency is given by $l(m\omega^2/EI)^{1/4}$. To produce Fig. 1, the infinite sum in Eq. (12) is truncated to a finite sum from $j = -50$ to $j = 50$. Fig. 1 shows that Eq. (8) produces the same results as those presented in Ref. [1].

### 2.3. Propagation wavenumber curves of a conventional ballasted track

For vertical dynamics of a railway track up to 3000 Hz, the Timoshenko beam model can be employed to model the rail. According to the Timoshenko beam theory, the differential equation of free vibration of the

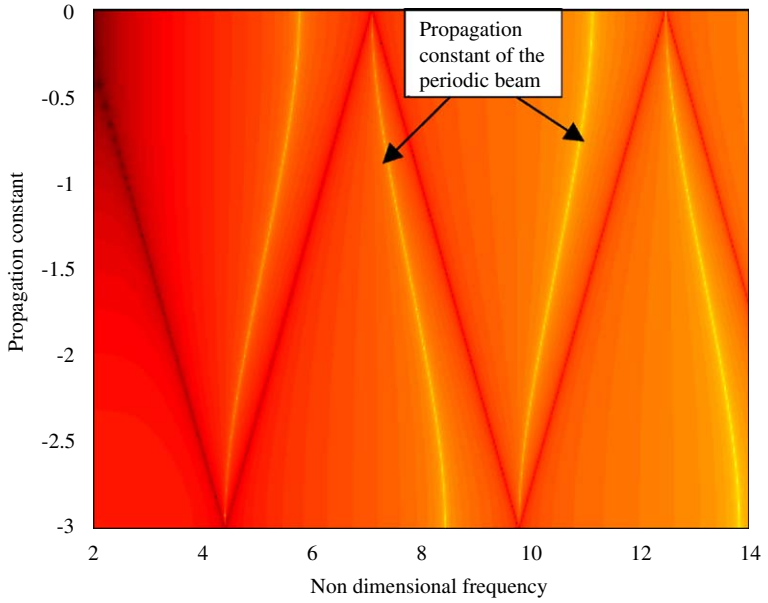


Fig. 1. Propagation constant of a periodic simply supported Euler beam.

rail without supports is given by

$$\rho A\frac{\partial^2 w}{\partial t^2}-\kappa AG\frac{\partial^2 w}{\partial x^2}+\kappa AG\frac{\partial \psi}{\partial x}=0, \tag{14}$$

$$\rho I\frac{\partial^2 \psi}{\partial t^2}-EI\frac{\partial^2 \psi}{\partial x^2}-\kappa AG\frac{\partial w}{\partial x}+\kappa AG\psi=0, \tag{15}$$

where $w$ is the vertical displacement of the rail and $\psi$ is the rotation angle of the cross-section due to the bending moment only. Each support consists of a railpad, a sleeper and ballast. The railpad and ballast are modelled as a spring and the sleeper as a mass. By ignoring the rotation of the sleeper about its axis, the receptance matrix of the support associating with the rail displacements, $w$ and $\psi$, is given by

$$[\mathbf{H}(\omega)]=\begin{bmatrix}\dfrac{k_{Bv}+k_{Pv}-m_S\omega^2}{k_{Pv}[k_{Bv}-m_S\omega^2]} & 0\\ 0 & \dfrac{12}{b_S^2 k_{Pv}}\end{bmatrix}, \tag{16}$$

where, $k_{Pv}$ and $k_{Bv}$ are stiffness of the railpad and ballast, $m_S$ is the sleeper mass and $b_S$ is the sleeper width.

Comparison of Eqs. (14) and (15) with Eq. (1) shows

$$\{q\}=\begin{Bmatrix}w\\ \psi\end{Bmatrix},\quad [\mathbf{M}]=\begin{bmatrix}\rho A & 0\\ 0 & \rho I\end{bmatrix},\quad [\mathbf{K}]_0=\begin{bmatrix}0 & 0\\ 0 & \kappa AG\end{bmatrix},$$
$$[\mathbf{K}]_1=\begin{bmatrix}0 & \kappa AG\\ -\kappa AG & 0\end{bmatrix},\quad [\mathbf{K}]_2=\begin{bmatrix}-\kappa AG & 0\\ 0 & -EI\end{bmatrix},$$

and $[\mathbf{K}]_3=[\mathbf{K}]_4=[0]$. Insertion of these matrices into Eqs. (6)–(8) yields the propagation wavenumber equation. When the track is treated as being continuously supported, the propagation wavenumber is given by Eq. (10).

The contour plots of $1/|\det([\mathbf{A}(\beta,\omega)])|$ and $1/|\det([\mathbf{A}_0(\beta,\omega)])|$ on the frequency–wavenumber plane are shown in Figs. 2 and 3, with the propagation constant curves and other characteristic curves being indicated. The values of the track parameters used here are from Ref. [3] and listed in Table 1. These parameters are for half the track structure (i.e., a single rail on half sleepers) and correspond to a track with concrete sleepers and

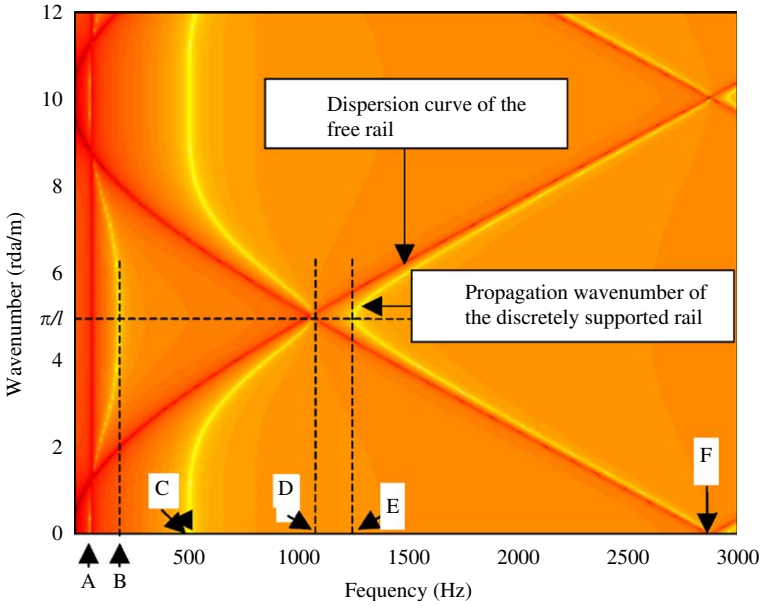


Fig. 2. Propagation wavenumber of the track as a periodic structure.

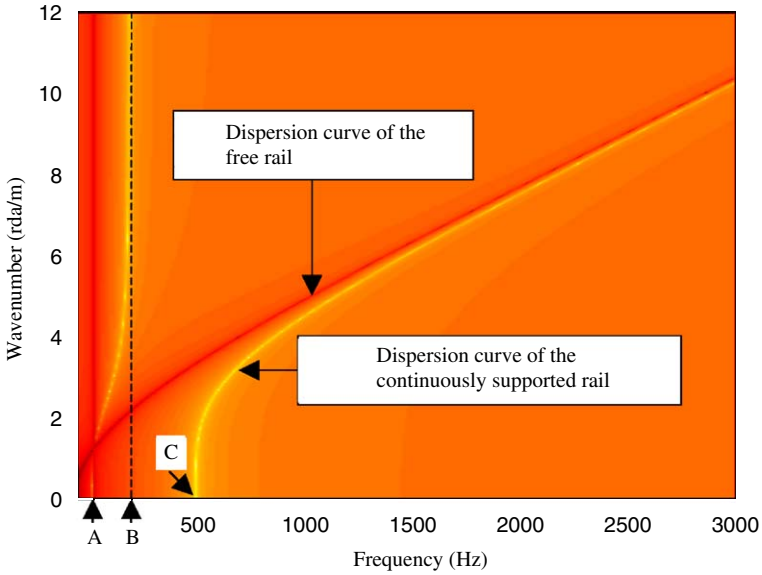


Fig. 3. Propagation wavenumber of the continuously supported track.

moderately stiff rail pads. Again, to produce Fig. 2, the infinite sum in Eq. (8) is truncated to a finite sum from $j = -50$ to $j = 50$. This finite sum is found to be sufficient.

## 3. Discussion

### 3.1. Stop and pass bands and bounding frequencies

Fig. 2 shows stop frequency bands (0-A, B-C and D-E) and pass frequency bands (A-B, C-D and E-F). Frequencies at A, B, C, D, E and F are about 80, 230, 520, 1070, 1300 and 2868 Hz. At these bounding frequencies, the propagation constants are either zero or $\pi$. These bounding frequencies can be calculated

Table 1
Parameters for the vertical dynamics of a track

| | |
|---|---|
| Density of the rail | $\rho = 7850\,\mathrm{kg/m^3}$ |
| Young's modulus of the rail | $E = 2.1 \times 10^{11}\,\mathrm{N/m^2}$ |
| Shear modulus of the rail | $G = 0.81 \times 10^{11}\,\mathrm{N/m^2}$ |
| Cross-sectional area of the rail | $A = 7.69 \times 10^{-3}\,\mathrm{m^2}$ |
| Second moment of area of the rail cross-section | $I = 30.55 \times 10^{-6}\,\mathrm{m^4}$ |
| Shear coefficient of the rail cross-section | $\kappa = 0.4$ |
| Vertical rail pad stiffness | $k_{Pv} = 3.5 \times 10^{8}\,\mathrm{N/m}$ |
| Mass of sleeper | $m_S = 162\,\mathrm{kg}$ |
| Sleeper spacing | $l = 0.6\,\mathrm{m}$ |
| Sleeper width | $b_S = 0.25\,\mathrm{m}$ |
| Vertical ballast stiffness | $k_{Bv} = 50 \times 10^{6}\,\mathrm{N/m}$ |

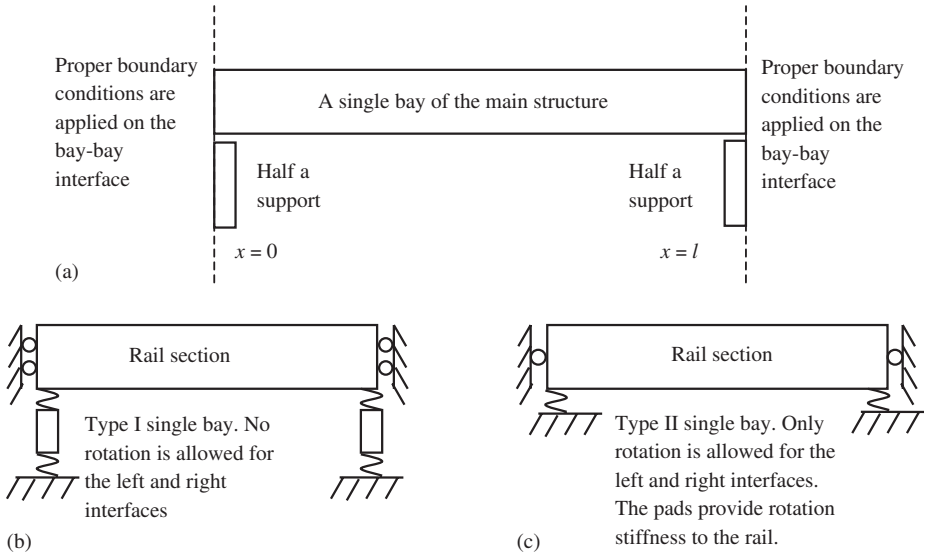


Fig. 4. (a) A single bay of the periodic structure; (b) the type I single bay of the track and (c) the type II single bay.

using a single bay from $x = 0$ to $x = l$ (Fig. 4(a)) of the periodic track structure with proper boundary conditions applied on the left and right bay–bay interfaces, as first identified in Refs. [5] and [6]. Since the periodic structure is symmetric about the bay–bay interface at any support (e.g. the support at $x = 0$), free vibrations are either symmetric or anti-symmetric about this bay–bay interface. This observation provides the basis for the determination of the bounding frequencies from an appropriate single bay, as discussed below.

When the propagation constant is zero, the free vibration at the bay–bay interface at $x = 0$ is equal to that at the bay–bay interface at $x = l$. If the free vibration is symmetric about $x = 0$, then the rotational displacements of the two interfaces of the single bay must be vanishing (or equivalently blocked) while their translational displacements are in-phase and at the same amplitude. In other words, the single bay displays a deformation pattern which is symmetric about the mid-span of the single bay. The single bay with the rotational displacements of the two interfaces being blocked is termed the *type I* single bay (Fig. 4(b)). If the free vibration of the periodic track structure is anti-symmetric about $x = 0$, then the vertical displacements of the two interfaces of the single bay must be blocked, but the rotational displacements are allowed and they are identical in both magnitude and direction. Thus the single bay presents a deformation pattern which is anti-symmetric about the mid-span of the bay. The single bay with the vertical displacements of the two interfaces being blocked is termed the *type II* single bay (Fig. 4(c)).

When the propagation constant is $\pi$, the free vibration of the periodic track structure at the bay–bay interface at $x = 0$ is equal in magnitude but opposite in direction to that at the bay–bay interface at $x = l$. If the free vibration is symmetric about $x = 0$, then the rotational displacements of the two interfaces of the single bay must be vanishing (or equivalently blocked to become the type I single bay) while their translational displacements are out of phase. In other words, the single bay presents a deformation pattern which is anti-symmetric about the mid-span of the bay. If the free vibration of the periodic track structure is anti-symmetric about $x = 0$, then the vertical displacements of the two interfaces of the single bay must be blocked (therefore becomes the type II single bay), while the rotational displacements are equal to each other in magnitude but opposite in direction. Thus the single bay presents a deformation pattern, which is symmetric about the mid-span of the bay.

Both of these two types of single bay defined above are finite structures and symmetric about the mid-span. The natural modes of such a finite structure are either symmetric or anti-symmetric about the mid-span. It can be concluded from the above two paragraphs that natural frequencies of the symmetric modes of the type I single bay and those of the anti-symmetric modes of the type II single bay are the bounding frequencies associating with zero propagation constant of the periodic structure. On the other hand, natural frequencies of the anti-symmetric modes of the type I single bay and those of the symmetric modes of the type II single bay are the bounding frequencies at which the propagation constant of the periodic structure is $\pi$.

### 3.2. Rail resonances at bounding frequencies and effect of load speed

In addition to the propagation wavenumber curves shown in Figs. 2 and 3, the magnitude of the ratio of the displacement of the rail at the loading point to a stationary or moving (at 80 m/s) vertical harmonic load is also shown here in Fig. 5 against load frequency. These curves are produced using the method presented in Ref. [3], and to account for damping in the track structure, loss factors of 0.25 and 1.0 are introduced, respectively, for rail pads and the ballast. For the stationary load, the ratio is just the driving point receptance which is independent of time but dependant on the loading position on the rail. Here, results are shown for two loading points, above a sleeper and at the mid-span. For the moving load however, the ratio is not a constant but a periodic function of time with period equal to the sleeper-passing time [3]. It contains not only

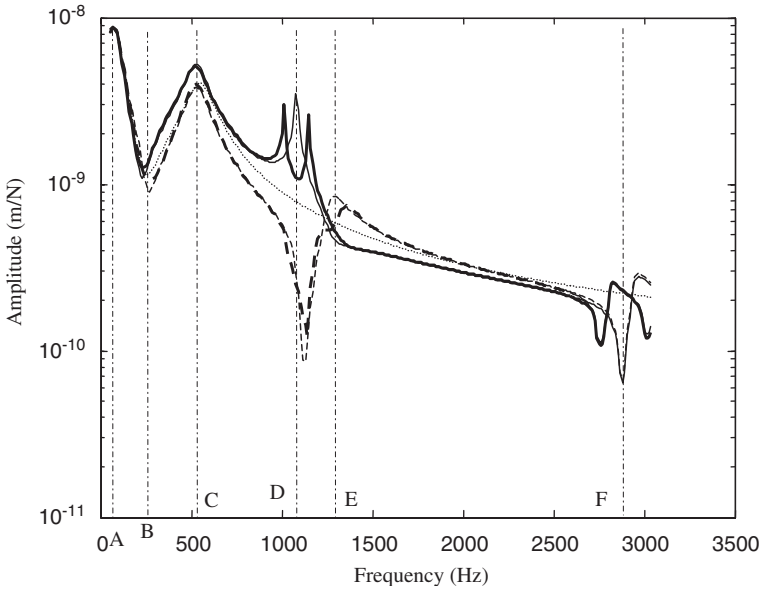


Fig. 5. Displacement-to-force ratio at the loading point due to a stationary or moving (80 m/s) load of different frequencies. Thin solid line, stationary load at mid-span; thin dashed line, stationary load above a sleeper. Thick solid line, moving load which passes the mid-span at time $t = 0$; thick dashed line, moving load which passes a sleeper at $t = 0$; dotted line, the load moving along or stationary on the continuously supported track.

the harmonic component at the sleeper-passing frequency, but also harmonic components at multiple sleeper-passing frequencies. The ratio is also dependant on the initial position (i.e., the position at $t = 0$) of the load. In Fig. 5, the ratio is plotted against load frequency for the instant $t = 0$ at which the moving load passes either the mid-span (thick solid line) or a sleeper (thick dashed line). A comparison of Fig. 2 with Fig. 5 shows resonances/anti-resonances of the rail at the bounding frequencies of the propagation constant curves.

The frequencies at A (about 80 Hz) and C (about 520 Hz) are the first and third natural frequencies of the type I single bay. The modes associating with these two frequencies are symmetric about the bay mid-span. The frequency at B (230 Hz) is the second natural frequency of the type I single bay and associates with an anti-symmetric mode. The modal shapes of the rail section are shown in Fig. 6. In the first mode, shown in Fig. 6(a), the rail section behaves like a rigid body and it vibrates in phase with the sleeper. In the second mode (Fig. 6(b)), the apparent motion of the rail section is negligible compared to those of the sleepers; however the small shear deformation of the rail section cause the natural frequency of this mode to be lower than what would be (250 Hz) if the rail were rigid. In the third mode (Fig. 6(c)), the rail section, vibration vertically with a small symmetric bending deformation, vibrates out of phase with that of the sleepers. The small bending deformation of the rail section also causes the natural frequency of this mode to be lower than what would be (548 Hz) if the rail were rigid. (If the rail is rigid, the type I single bay is a system of three-degree-of-freedom (vertical displacements of the rail, the left sleeper and the right sleeper)). Thus, at A and C the rail has a peak frequency response for both the mid-span and above a sleeper and at B, the rail presents a dip response, as shown in Fig. 5. For the continuously supported rail (Fig. 3), frequencies (A and C) associating with a zero wavenumber are the natural frequencies (which are evaluated to be about 80 and 548 Hz) of the track system with the rail having an infinitely long wavelength (i.e., the rail behaves as rigid). The frequency (B) associating with an infinite large wavenumber is the resonance frequency (250 Hz) of the sleepers on their supports (rail and ballast).

The frequency at D (about 1070 Hz) in Figs. 2 and 5 is the first natural frequency of the type II single bay shown in Fig. 4(c). This is a symmetric mode (Fig. 7(a)) of the type II single bay in which the rail has no vertical displacement at sleepers but reaches the maximum vertical displacement at mid-span. This frequency is often termed the first pinned–pinned frequency and the mode is termed the first pinned–pinned mode. It can be seen that, the pinned–pinned frequency is almost independent of the support (since the rotation stiffness from the pad to the rail is very small) and therefore cannot be changed by for example changing the pad stiffness. A stationary harmonic load at this frequency will excites this mode, thus the driving point receptance of the rail has a peak when the load is applied at the mid-span and a dip when it is applied above a sleeper, as

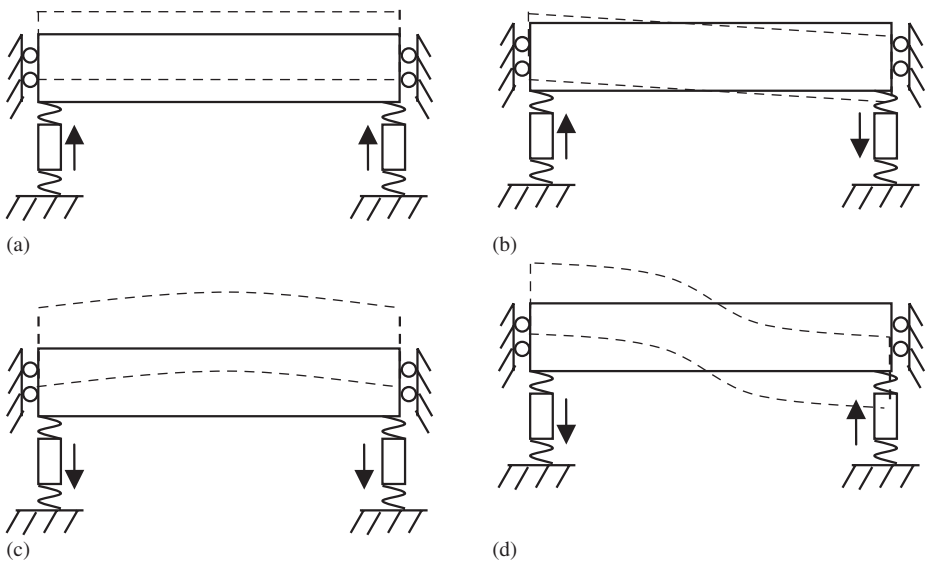


Fig. 6. Mode shapes (in dashed line) of the rail section of the type I single bay (the arrows indicate the sleeper displacement): (a) the first mode; (b) the second mode; (c) the third mode and (d) the fourth mode.

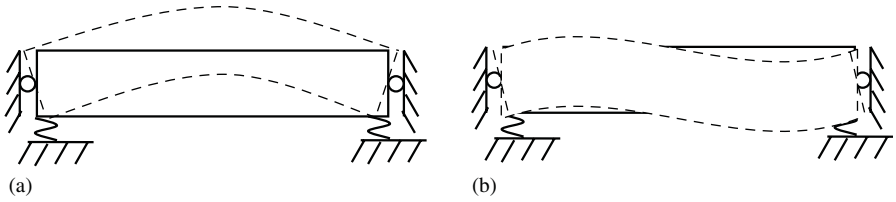


Fig. 7. Mode shapes (in dashed line) of the rail section of the type II single bay: (a) the first mode and (b) the second mode.

shown in Fig. 5. For a moving harmonic load however, the pinned–pinned mode is excited at two other frequencies: one (denoted by $f_u$) is higher than the pinned–pinned frequency and the other (denoted by $f_l$) is lower. This phenomenon is indicated in Fig. 5 by the splitting of the single peak for the stationary load into two lower peaks for the moving load. This can be explained as the Doppler effect and these two frequencies can be determined by

$$f_{l,u} = f_{\text{pinned}-\text{pinned}} \mp c/2l, \tag{17}$$

since at the pinned–pinned frequency, the propagation wavenumber is $\pi/l$. At 80 m/s, $f_l = 1070 - 67 = 1003$ Hz and $f_u = 1070 + 67 = 1137$ Hz Hz. Frequency difference between the two sub-peaks is 134 Hz.

If wheels move along an irregular rail such that the excitation frequency (wheel speed divided by roughness wavelength) is within the interval $[f_{\text{pinned}-\text{pinned}}, f_u]$, propagating modes near or at the first pinned–pinned frequency will be excited. The forced vibration will propagate along the rail to a larger distance since the mode excited is close to a mode of the free rail (Fig. 2 shows an intersection at the pinned–pinned frequency of the dispersion curve of the free rail and the propagation constant curve of the track). This vibration propagation enhances rail-radiated noise and interactions between the wheels. However, if the moving of the wheels is replaced with the moving of the roughness strip, as done by many researchers, then no propagation mode is excited since the excitation frequency is within a stop band. The vibration of the rail decays quickly along either sides of a wheel, producing rail-radiated noise and wheel–wheel interactions which are significantly different from the actual situation. By comparing excitation frequency and the changing rate of the loading point displacement, Ref. [3] has already shown that, for excitation frequencies higher than 200 Hz, the 'moving roughness' approach will produce significant errors in wheel/rail interaction calculations, especially near the pinned–pinned frequency. This is now further confirmed here by considering vibration propagation.

In dealing with interactions between moving wheels and a rough rail, some researchers use a quasi-static approach (e.g., Refs. [7,8]). According to this approach, the track provides a varying dynamic stiffness as a load moves. In the calculation of the varying stiffness of the track, $x = ct$ (where $c$ is the speed of the moving load) is set into the receptance, $\alpha_p(x, \omega)$, of the rail at the loading point, $x$, due to a unit *stationary* harmonic load of frequency $\omega$, and then the receptance is inversed to give the time-dependent stiffness of the track. As discussed in the last paragraph, the quasi-static approach is invalid at least in the frequency range of $[f_{\text{pinned}-\text{pinned}}, f_u]$, since a propagating vibration caused by a moving load is replaced by a non-propagating vibration.

The frequency at E (1300 Hz) in Figs. 2 and 5 is the 4th natural frequency of the type I single bay. This frequency is influenced by the support: by increasing pad stiffness, this frequency will be increased and the associated stop band becomes wider. The modal shape of the rail section is shown in Fig. 6(d). The mode involves an anti-symmetric deformation of the rail section about the mid-span: the rail has a maximum vertical displacement above a sleeper (therefore a peak frequency response in Fig. 5) and no vertical displacement at mid-span. The peak is also split and lowered by the moving load.

The frequency at F (2868 Hz) in Figs. 2 and 5 is the 2nd natural frequency of the type II single bay. This frequency is also determined by the rail only. The mode, shown in Fig. 7(b), involves an anti-symmetric deformation of the rail section about the mid-span of the single bay. Thus, in this mode (termed the second pinned–pinned mode), the rail has no vertical displacement at the mid-span and above a sleeper. That is why a dip is present in the stationary-forced response of the rail (Fig. 5) for both of these two positions. The dip is split into two sub-dips by the moving load and the frequency difference of these two sub-dips is given by $2c/l$,

which is 267 Hz at 80 m/s. Again, the 'moving roughness' approach and the quasi-static approach have problems in the frequency range of 267 Hz centred at the second pinned–pinned frequencies.

## 4. Conclusion

In this short communication, the usefulness of a general propagation constant equation derived in a previous paper is demonstrated by producing propagation constant curves for an Euler beam on periodically repeated simple supports and for a conventional ballasted track. A detailed discussion then follows on the track propagation and resonance behaviours. At the bounding frequencies of the pass and stop bands of the periodic track structure, the propagation constants are either zero or $\pi$. At these frequencies, the rail subject to a vertical harmonic load either resonates or anti-resonates. By associating the bounding frequencies with the natural modes of a single bay of the track, characteristics of the frequency response of the track, including resonances/anti-resonances of the rail at the bounding frequencies and the splitting of a peak or dip due to a moving load, are well explained and understood. The 'moving roughness' approach and the quasi-static approach in modelling wheel/rail interactions are further shown to be problematic since these approaches, in addition to other aspects, assume a different propagation characteristics at certain frequencies. To overcome the shortcomings of these approaches, a new method has been developed and will appear in a separate paper.

## References

[1] D.J. Mead, Wave propagation in continuous periodic structures: Research contributions from Southampton, *Journal of Sound and Vibration* 190 (1996) 495–524.
[2] L. Gry, C. Gontier, Dynamic modelling of railway track: a periodic model based on a generalised beam formulation, *Journal of Sound and Vibration* 199 (1997) 531–558.
[3] X. Sheng, C.J.C. Jones, D.J. Thompson, Responses of infinite periodic structures to moving or stationary harmonic loads, *Journal of Sound and Vibration* 282 (2004) 125–149.
[4] L. Gavric, Finite element computation of dispersion properties of thin-walled waveguides, *Journal of Sound and Vibration* 173 (1994) 113–124.
[5] D.J. Mead, Wave propagation and natural modes in periodic systems: I. Mono-coupled systems, *Journal of Sound and Vibration* 40 (1975) 1–18.
[6] D.J. Mead, Wave propagation and natural modes in periodic systems: II. Mono-coupled systems, with and without damping, *Journal of Sound and Vibration* 40 (1975) 19–39.
[7] A. Nordborg, Wheel/rail noise generation due to nonlinear effects and parametric excitation, *Journal of Acoustical Society of America* 111 (2002) 1772–1781.
[8] T.X. Wu, D.J. Thompson, On the parametric excitation of wheel/track system, *Journal of Sound and Vibration* 278 (2004) 725–747.